Infrared Interferometric observation of dust in the nuclei of active galaxies

Raban, D.

Chapter 5

Resolved infrared emission from the QSO 3C 273

Abstract. In order to detect emission from a putative dusty torus, we obtained spectro-interferometric observations of the QSO 3C 273 with the MIDI instrument at the VLTI, in the wavelength range 7-11 μm. Two visibility measurements were obtained at similar baseline length (~ 35m) but at nearly perpendicular position angles. These measurements have been supplemented by VISIR N-band photometry and Spitzer spectrum.
Combined, these measurements show the infrared emission to be resolved with a projected size of 32 $\times$ 84 parsec. We also tentatively detect the 10μm silicate feature in emission in one of the correlated spectra. The spatial scale of the mid-infrared emission agrees with the luminosity-radius relation for the dusty torus in AGN. Therefore we conclude that the obscuring torus commonly found in Seyfert 2 nuclei and predicted by the AGN unification model can therefore also be present in type 1 sources such as 3C 273.

5.1 Introduction

In the standard model for Active Galactic Nuclei (AGNs), the central black hole, accretion disk and broad line region are surrounded by a thick, torus-shaped structure of dust: the obscuring torus. The torus absorbs UV photons from the accretion disk and re-emits the energy in the mid-infrared. Infrared observations are the obvious way to directly observe the obscuring torus, but conventional single-dish observations are unable to resolve the structure. The situation has changed with the introduction of near- and mid-infrared interferometers such as the Keck interferometer and the Very Large Telescope Interferometer (VLTI). These interferometers are able to resolve the dusty structure at the milliarcseconds scales, allowing for direct measurement of the properties of the dusty torus. The observations presented here are part of an ongoing campaign to detect tori with the Mid InfrareD Interferometer (MIDI), which is coupled to the VLTI. Previous observations of nearby Seyfert galaxies revealed the presence of parsec-scale dust distributions in the centres of those galaxies, much in agreement with the standard model (Jaffe et al. 2004; Meisenheimer et al. 2007; Tristram et al. 2007; Raban et al. 2009; Tristram et al. 2009). With the data presented here, we extend our sample of active galaxies to include a non-nearby, high luminosity object, the Quasar 3C 273.

3C 273 is a radio-loud quasar with redshift z=0.158 (Strauss et al. 1992) at a distance of $\sim 650 h^{-1}$ Mpc ($H_0 = 73\,\mathrm{km\,s^{-1}\,Mpc^{-1}}$, 1pc=0.3 mas). It is one of the most studied objects of its type, being the brightest quasar on the sky and the first one to be discovered (Schmidt 1963).

At millimetre and infrared wavelengths, the object's continuum spectral energy distribution is characterised by a power law of index 0.7 ± 0.1 (Courvoisier 1998). Thermal emission is also suspected as the presence of a 3μm bump was interpreted early on as evidence of the presence of hot dust (Neugebauer et al. 1979; Allen 1980). Robson et al. (1993) and Paltani et al. (1998) have established the presence of at least two components to the thermal infrared emission from 3C 273. Recently, due to a historical minimum in the synchrotron emission from the jet, Türler et al. (2006) identify three thermal (and unresolved) dust emission components in the infrared spectrum, with temperatures $\sim 45, 300$ and 1500 K.

3C 273 is notable for its extreme variability, with large variations at the millimetre and the infrared bands. For example, at infrared wavelengths unprecedented variations have been detected in 1988 (Courvoisier et al. 1988), when the infrared flux at 4.8, 10, 20 μm changed by a factor of two on a timescale as short as one day. The flux density measurements of the 1988 flare in the infrared fits a power-law spectrum with a spectral index of 1.2 ($f_\nu \sim \nu^{-\alpha}$). Paltani et al. (1998) identified two variable components as responsible for the short and long term variations, one associated with the accretion disk, and the other with the inner jet. However, the extreme variability of the source has been and still is unaccounted for, as has been noted by Robson et al. (1993) and Paltani et al. (1998), as well as others.

The 10μm silicate feature in emission was detected by the Spitzer space telescope (Hao et al. 2005). This emission supports the presence of centrally heated dust viewed face-on. Due to Spitzer's low spatial resolution, however, we do not know the size of

the silicate emitting region, or whether it is indeed related to the obscuring torus.

Correlations between the near-IR and the optical-UV emission (Soldi et al. 2008) find a lag of 0.8-1.2 years, corresponding to a distance of 0.24 - 0.35 parsecs, which may represent the light travelling time from the UV source to the dust location, i.e. the inner radius of the torus.

The main goal of this paper is to determine the nature of the infrared emission from 3C 273 at milliarcseconds resolution, and in particular to detect thermal emission from the putative torus predicted by AGN unification models, and to compare our findings with the predictions of the AGN unification model.

This paper is organised as follows. Section 5.2 describes the observations and data reduction procedures. In §6.4 we describe the results of the measurements. In §6.5 we discuss the size constraints, detection of the silicate emission feature, implications on AGN unification models, dust emission mechanism, variability, and the relative orientations of the dust and the jet. A summary and conclusions is presented in §5.5

5.2 Instrument, observations and data reduction

5.2.1 Observations

Spectro-Interferometric: MIDI is a classical Michelson interferometer, combining two beams from two 8.2m unit telescopes, after dispersing the beams using a prism. For a detailed description of the instrument see Leinert et al. (2003).

3C 273 was observed with MIDI on February 07, 2007 with a baseline length (BL) of 37m and position angle (PA) of 31° and April 21, 2008 (BL=30m, PA=128°). The obtained spectral resolution is $R = \lambda/\delta\lambda \simeq 30$. The correlated fluxes are normally accompanied by single-dish measurement of the flux of the source. During the data reduction these are then used to determine the visibility of the source and provide additional constraints on the size and emission mechanism. Due to technical difficulties we could not measure the single dish flux, only the correlated fluxes. In stead, we use data from the Spitzer Space Telescope accompanied by VISIR photometry to estimate the single dish flux. Both are described below.

Data was reduced with the EWS (Expert Work Station) reduction package (Jaffe 2004). In addition to standard reduction procedures, and in order to increase the signal to noise in the correlated fluxes, we estimated the level of noise by looking at frames where no interferometric signal was detected. These noise levels where then removed from the data.

Photometric: To obtain a rough estimate for the total flux of the source, intermediate band photometry with VISIR was obtained on March 1, 2007, 23 days after the first interferometric observation. VISIR, the VLT Imager and Spectrometer for the mid-InfraRed, provides a long-slit spectrometer as well as a high sensitivity imager in both the N and the Q bands. The two filters in which 3C 273 was observed were PAH1 ($\lambda_0 = 8.59\,\mu$m, $\Delta\lambda = 0.42\,\mu$m) and SiC ($\lambda_0 = 11.85\,\mu$m, $\Delta\lambda = 2.34\,\mu$m). The calibrator star for the VISIR observations was HD 124294. The VISIR data were reduced by combining the chopped and nodded frames in the standard procedures for such data. The photometry was extracted in a 2.25 arcsec aperture. For the calibration, the template spectrum of HD 124294 from the catalogue by Roy van Boekel (private comm.) was

used.

In addition, we used Spitzer data in order to compare the flux of Spitzer to the VISIR data and the correlated fluxes. The Spitzer data was obtained on two different dates: 2007 Feb 28 (one day before the observations with VISIR) and 2007 Jun 28, to which the 2005 Spitzer data of Hao et al. (2005) was added. All sets show within 10% an almost identical spectrum.

5.3 Results

The correlated fluxes as a function of wavelength, VISIR photometry and Spitzer spectra are displayed in Figure 5.1.

5.3.1 MIDI

The correlated flux of Feb. 4, 2007 rises with wavelength from 0.18 ± 0.02 Jy at 7μm to 0.35± 0.02 Jy at 11 μm. At the shorter wavelength end it is 30% lower than the Spitzer spectrum and the VISIR photometry. At 10-11 μm, the Feb. 4 correlated flux matches the Spitzer data. The source is therefore resolved in this case at shorter wavelengths only, where the spatial resolution is highest.

The correlated flux of April 22 ,2008 rises from 0.1± 0.02 Jy at 7 μm to 0.2± 0.02 Jy at 11 μm. Although is was taken with a shorter baseline (30m, as opposed to 37m for the Feb. 4 correlated flux), the correlated flux of April 22 in considerably lower. The difference between the two correlated fluxes is most likely due to the source having an elongated morphology, which is more extended towards PA=128°.

5.3.2 VISIR & Spitzer

In the VISIR images (not shown) the flux is contained within 1.5 arcsec and the FWHM of the PSF is 0.39 arcsec and 0.44 arcsec at 8.59 μm and 11.85 μm, respectively. This is only not significantly larger than the FWHM of the (unresolved) calibrator star. 3C 273 is hence not resolved by the VISIR imaging.

The Spitzer spectra is fully consistent with the VISIR photometry, as expected from an unresolved source, indicating that the mid-IR flux was stable over the period of the measurements. We therefore use the Spitzer spectrum to derive visibilities (and therefore size estimates) for both correlated fluxes.

Additional MIDI data acquired in May 2009 in DDT observations confirm the 2008 values for the total fluc.

5.4 Discussion

5.4.1 size constraints

The difference between the correlated fluxes indicates an elongated morphology for the source. In order to model both sets of data with a single elongated source model, at least three parameters are needed: the major and minor axis sizes and the position angle. With two data point we cannot unambiguously apply a single model of an elongated source. We therefore fit the two correlated fluxes independently. First, we derive

Table 5.1. Derived projected sizes for the mid-infrared emission

projected baseline degrees	FWHM mas	FWHM pc
31°	10.2 $\pm$4	32 $\pm$12
128°	27 $\pm$4	84 $\pm$12

visibilities for both correlated fluxes by dividing them by the Spitzer data. The resulting visibilities are displayed in Figure 5.2. Next, we fit the resulting visibilities with a model of a Gaussian flux distribution. With no prior information on the morphology of the source, a Gaussian model is the most general among the different modelling options, and is able to constrain the characteristic size of the emitter regardless of its actual shape. The source size, projected on a baseline with PA=31° is 10.2$\pm$4 mas, which translates to 32$\pm$12 parsec at the distance to the source. The size projected on a baseline with PA=128° is 27 ± 4 mas, which translate to 84 ± 12 parsec. The visibility fits to the data are shown in Figure 5.2, and the derived sizes are noted in Table 5.1.

5.4.2 A possible silicate feature in emission

The convex shape of the Feb. 28 correlated flux suggests the presence of the 10 μm silicate feature in emission. Due to the limited spectral range of MIDI we do not measure the full extent of the feature, nor we can separate the silicate emission from the underlying continuum, as has been done with Spitzer data by Hao et al. (2005). The same shape does not appear on the second correlated flux. A similar result was found in MIDI observations of the Seyfert 1 nucleus of NGC 4151 (Burtscher et al, in preparation), which was also observed with two u-v points, and showed a weak silicate feature in emission for the baseline observation which was less resolved. The tentative nature of the detection of the silicate feature in both cases makes it quite hard to draw robust conclusions. Further analysis must wait for more observations.

5.4.3 Implications on the AGN unification model

Here we compare our findings with specific predictions made by the standard AGN unification model, with additional insight from current state of the art simulations of clumpy tori. The standard model predicts the appearance of the 10μm silicate feature in emission in the case of a face-on torus (Pier & Krolik 1992). The lack of detection of the feature was considered a major drawback in accepting the standard model. In 2005, the silicate feature in emission was detected in a handful of objects, mostly PG quasars (Hao et al. 2005; Siebenmorgen et al. 2005) , including 3C 273. Our tentative detection of the silicate emission feature is then fully consistent with unification models.

The standard model relates in theory the inner (sublimation) radius of the torus, R_d, to the luminosity of the central engine (Nenkova et al. 2008):

$$R_d \simeq 0.4 \left(\frac{L}{10^{45}\,\mathrm{erg\,s^{-1}}} \right)^{1/2} \left(\frac{1500\,K}{T_{sub}} \right)^{2.6} \mathrm{pc}. \tag{5.1}$$

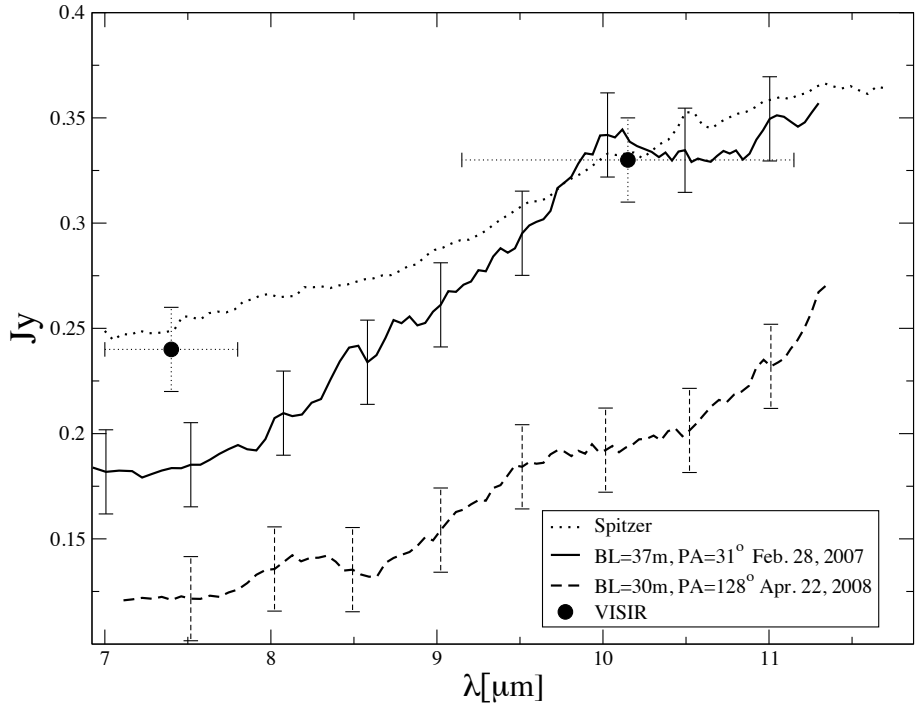

Figure 5.1 — Redshift-corrected correlated fluxes, Spitzer and VISIR data. Solid: Feb. 28, 2007 correlated flux. Dashed: April 22, 2008 correlated flux. Dotted: Spitzer Spitzer spectrum of Hao et al. (2005). Filled circles: VISIR photometry.

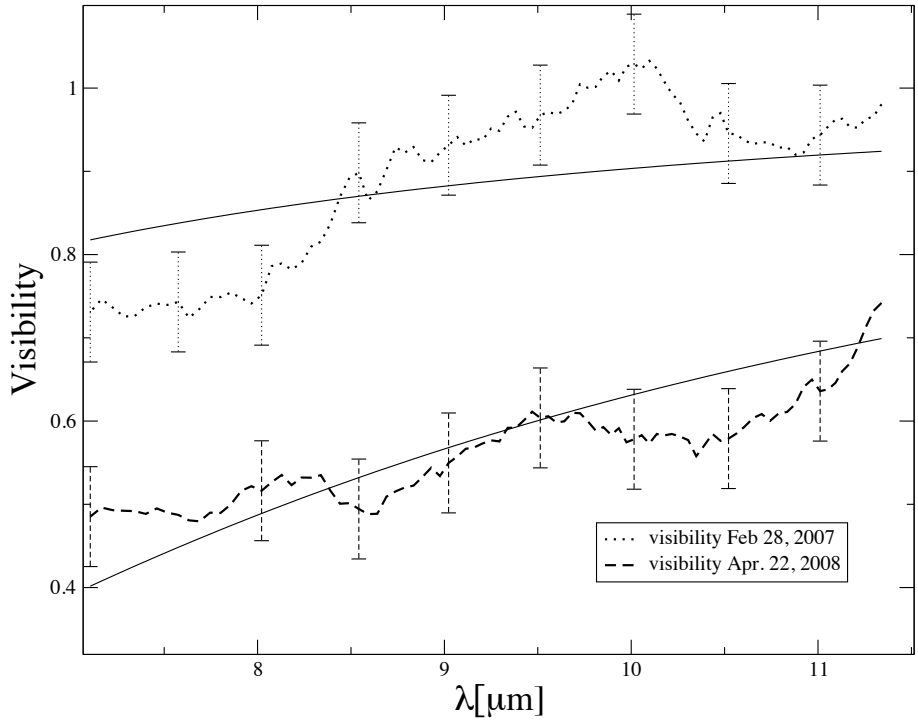

Figure 5.2 — Visibilities for the two u-v points and model fits. Dotted: data from Feb.8, 2007. Dashed: data from April 22, 2008. Solid: model fits to the data

For 3C 273, the central engine luminosity is $\sim 10^{47}$ erg s^{-1} (Hao et al. 2005), which translates to a size of 4 pc for the sublimation radius of the dust, assuming a sublimation temperature of 1500 K, typical of many dust species. Further, recent three dimensional radiative transfer simulations of clumpy media (Nenkova et al. 2008; Schartmann et al. 2008) conclude that the outer radius of the torus is $\sim$10 times its inner radius, in our case 40 pc. The projected size of the structure resolved by MIDI is, then, of the same order of magnitude as predicted from simulations. Thus, based on the size estimates given the luminosity of the source, we identify the resolved structure with the obscuring torus of the AGN unification models, and our findings are quite consistent with the predictions of such models.

5.4.4 Elongation and the inclination of the jet

An upper limit on the inclination of the jet in 3C 273 can be derived from the apparent super-luminar motion of the jet. The fastest radial jet speed measured for this object is $\beta = 13.4c$ (Lister et al. 2009). The upper limit on the viewing angle is then: $\theta < 2 \arctan \beta^{-1} = 8.5°$.

The inclination of the jet raises the question of how to interpret the elongation we detect with MIDI. Simplistic (and likely naive) views on AGNs consider the obscuring torus to be perpendicular to the jet and circularly symmetric. In that respect, the inclination of the jet implies a nearly completely face-on torus, which should appear symmetric under the assumptions mentioned above. there are at least three mechanism which could produce an elongated appearance to the torus in 3C 273:

1. **Inclination of the dust with respect to the jet**. An elongated structure may appear if the axis of the torus is not perpendicular to the jet. Although at odds with the simplistic view of AGN, there is now a growing body of evidence which strongly suggests that this is, in fact, the general case: Statistically, Kinney et al. (2000) found little or no correlation between the relative angle of jets and the dust residing in the galactic disk for Seyfert galaxies. For individual objects, only two objects have data which directly relates the torus and the jet. The Seyfert 2 galaxy NGC 1068 has a dust distribution which is misaligned with the jet by $45°$ (Raban et al. 2009), while Circinus shows a dust distribution which is perpendicular to the jet (Tristram et al. 2007).
2. **An intrinsically elongated dust distribution**. Here, the dust structure itself possesses an elongation intrinsically. Although current theoretical models assume circular symmetry for the torus, this is mainly to simplify computation rather than a statement about the physical properties of the torus. In reality, there is neither an empirical nor a theoretical reason for the dust to be circular-symmetric. If the dust is accreted from circum-nuclear material (e.g. Schartmann et al. (2008)), then the dust might well be elongated in the direction from which it is fed. In the competing scenario (e.g. Elitzur & Shlosman (2006)), the exact morphology of the torus is determined by the little understood process of disk wind. Again, there is no reason to assume any symmetry as a result of this process. An elongated dust distribution is fully consistent with current knowledge of the obscuring torus.
3. **An unequal illumination of the torus.** The morphology and distribution of clouds in the broad line region (BLR) is not yet known, due to the compact size

of the BLR. Nevertheless, it is not unlikely that the distribution of clouds and the optical depth of the clouds are not symmetric about the nucleus. Some of the UV radiation from the accretion disk could be absorbed by the BLR, resulting in unequal illumination and temperature profile. Since MIDI observes dust at a certain temperature, those differences could appear to us an an elongation.

To conclude, any of the above mentioned scenarios (or a combination of them) could take place in an AGN. In light of this discussion, the elongation of the dust with respect of the inclination of the jet is not surprising.

5.4.5 Emission mechanism

Our findings are fully consistent with thermal emission from the obscuring torus as the dominant emission mechanism. However, we now briefly consider and dismiss the possibility that the correlated fluxes arise from synchrotron emission from the base of the jet. Radio data from the MOJAVE[1] program show extended structures in the core of 3C 273, of a size ~ 20 mas, quite similar to the size we report here. The elongated 2 cm structures, however, appear oriented at position angle PA=$\sim -50^{\circ}$, a perpendicular PA compared to the structure seen by MIDI, which are elongated towards PA=$\sim 128^{\circ}$. We conclude that the PA of the 2 cm emission is incompatible with the MIDI data.

Another indication that the emission from 3C 273 is thermal comes from the similarity between the shape of the 3C 273 correlated fluxes and the shapes of the correlated fluxes of type 1 sources observed in the MIDI snapshot survey (Tristram et al. 2009).

5.4.6 Variability

The above discussion, and in particular the derived projected sizes of the source, all assume that the emission from the source is constant in time, and therefore the differences in the correlated fluxes are a result of the morphology of the source. As mentioned in the introduction, the variability of 3C 273 has been well studied. In the infrared, variations of a factor 2 in flux were observed within a day (Courvoisier et al. 1988). Since our observations were obtained 1.5 years apart, which similar to the time lags between the correlations of the optical/UV and the infrared, we cannot neglect the possibility that at least some, if not all of the differences in correlated flux are a result of the variability of the source. Specifically, the differences in the correlated fluxes might result from the variability of a compact, unresolved source, for example thermal emission from the accretion disc or synchrotron from the base of the jet. As already mentioned in Tristram et al. (2009), there are indications that there were no long term (within a time-scale of years) variations in the infrared spectrum of 3C 273. Moreover, we have examined X-ray monitor RXTE data (averaged over 100 days) over the period 2006-2009. We find that the 2008.3 nuclear X-ray counts from 3C273 was *higher* than in 2007.3, thereby making less likely the possibility that long-term variability is responsible for the differences between the correlated fluxes. However, the possibility of extremely short time-scale variations (a few hours) cannot be fully discounted, given the behaviour of the source in the past.

[1]Monitoring Of Jets in Active galactic nuclei with VLBA Experiments, Lister et al. (2009)

5.5 Summary and conclusions

We have presented spectro-interferometric and photometric observations of the quasar 3C 273. Assuming the source was not significantly variable in the considered period, the two interferometric measurements of the 7-11 μm correlated fluxes, taken 14 month apart, reveal the source to be resolved with sizes of 32, 84 parsec projected on baselines with position angles of 31°, 128°, respectably. The 10 μm silicate feature in emission is tentatively detected in on of our correlated fluxes. We identify the resolved structure with the obscuring torus of AGN unification model.

Acknowledgements

This research was supported by the Netherlands Organisation of Scientific Research (NWO) through grant 614.000.414. Based on observations collected at the European Southern Observatory, Chile. This research has made use of data from the MOJAVE database that is maintained by the MOJAVE team (Lister et al., 2009, AJ, 137, 3718).

References

Allen D. A., 1980, Nature, 284, 323
Courvoisier T. J.-L., 1998, A&A Rev., 9, 1
Courvoisier T. J.-L., Robson E. I., Hughes D. H., Blecha A., Bouchet P., Krisciunas K., Schwarz H. E., 1988, Nature, 335, 330
Elitzur M., Shlosman I., 2006, Astrophys. J., 648, L101
Hao L., Spoon H. W. W., Sloan G. C., Marshall J. A., Armus L., Tielens A. G. G. M., Sargent B., van Bemmel I. M., Charmandaris V., Weedman D. W., Houck J. R., 2005, Astrophys. J., 625, L75
Hönig S. F., Beckert T., Ohnaka K., Weigelt G., 2006, Astron. & Astrophys., 452, 459
Jaffe W., Meisenheimer K., Röttgering H. J. A., Leinert C., Richichi A., Chesneau O., Fraix-Burnet D., Glazenborg-Kluttig A., Granato G.-L., Graser U., Heijligers B., Köhler R., Malbet F., Miley G. K., Paresce F., Pel J.-W., Perrin G., Przygodda F., Schoeller M., Sol H., Waters L. B. F. M., Weigelt G., Woillez J., de Zeeuw P. T., 2004, Nature, 429, 47
Jaffe W. J., 2004, in Traub W. A., ed., Society of Photo-Optical Instrumentation Engineers (SPIE) Conference Series Vol. 549, pp 715–+
Kinney A. L., Schmitt H. R., Clarke C. J., Pringle J. E., Ulvestad J. S., Antonucci R. R. J., 2000, Astrophys. J., 537, 152
Meisenheimer K., Tristram K. R. W., Jaffe W., Israel F., Neumayer N., Raban D., Röttgering H., Cotton W. D., Graser U., Henning T., Leinert C., Lopez B., Perrin G., Prieto A., 2007, Astron. & Astrophys., 471, 453
Leinert C., Graser U., Przygodda F., Waters L. B. F. M., Perrin G., Jaffe W., Lopez B., Bakker E. J., Böhm A., Chesneau O., Cotton W. D., Damstra S., de Jong J., Glazenborg-Kluttig A. W., Grimm B., Hanenburg H., Laun W., Lenzen R., Ligori S., Mathar R. J., Meisner J., Morel S., Morr W., Neumann U., Pel J.-W., Schuller P., Rohloff R.-R., Stecklum B., Storz C., von der Lühe O., Wagner K., 2003, *Astrophysics and Space Science*, 286, 73
Lister M. L., Aller H. D., Aller M. F., Cohen M. H., Homan D. C., Kadler M., Kellermann K. I., Kovalev Y. Y., Ros E., Savolainen T., Zensus J. A., Vermeulen R. C., 2009, Astron. J., 137, 3718
Lister M. L., Homan D. C., Kadler M., Kellermann K. I., Kovalev Y. Y., Ros E., Savolainen T., Zensus J. A., 2009, Astrophys. J., 696, L22
Nenkova M., Sirocky M. M., Nikutta R., Ivezić Ž., Elitzur M., 2008, Astrophys. J., 685, 160
Neugebauer G., Oke J. B., Becklin E. E., Matthews K., 1979, Astrophys. J., 230, 79
Paltani S., Courvoisier T. J.-L., Walter R., 1998, Astron. & Astrophys., 340, 47
Pier E. A., Krolik J. H., 1992, Astrophys. J., 401, 99
Raban D., Jaffe W., Röttgering H., Meisenheimer K., Tristram K. R. W., 2009, Mon. Not. R. Astron. Soc., 394, 1325
Robson E. I., Gear W. K., Brown L. M. J., Courvoisier T. J.-L., Smith M. G., 1986, Nature, 323, 134
Robson E. I., Litchfield S. J., Gear W. K., Hughes D. H., Sandell G., Courvoisier T. J.-L., Paltani S., Valtaoja E., Terasranta H., Tornikoski M., Steppe H., Wright M. C. H., 1993, Mon. Not. R. Astron. Soc., 262, 249
Schartmann M., Meisenheimer K., Camenzind M., Wolf S., Tristram K. R. W., Henning T., 2008, Astron. & Astrophys., 482, 67
Schmidt M., 1963, Nature, 197, 1040
Siebenmorgen R., Haas M., Kruegel E., Schulz B., 2005, Astronomische Nachrichten, 326, 556
Soldi S., Türler M., Paltani S., Aller H. D., Aller M. F., Burki G., Chernyakova M., Lähteenmäki A., McHardy I. M., Robson E. I., Staubert R., Tornikoski M., Walter R., Courvoisier T. J.-L., 2008, Astron. & Astrophys., 486, 411
Strauss M. A., Huchra J. P., Davis M., Yahil A., Fisher K. B., Tonry J., 1992, ApJ, 83, 29
Tristram K. R. W., Meisenheimer K., Jaffe W., Schartmann M., Rix H.-W., Leinert C., Morel S., Wittkowski M., Röttgering H., Perrin G., Lopez B., Raban D., Cotton W. D., Graser U., Paresce F., Henning T., 2007, Astron. & Astrophys., 474, 837
Tristram K. R. W., Raban D., Meisenheimer K., Jaffe W., Röttgering H., Burtscher L., Cotton W. D., Graser U., Henning T., Leinert C., Lopez B., Morel S., Perrin G., Wittkowski M., 2009, ArXiv e-prints

Türler M., Chernyakova M., Courvoisier T. J.-L., Foellmi C., Aller M. F., Aller H. D., Kraus A., Krichbaum T. P., Lähteenmäki A., Marscher A., McHardy I. M., O'Brien P. T., Page K. L., Popescu L., Robson E. I., Tornikoski M., Ungerechts H., 2006, Astron. & Astrophys., 451, L1